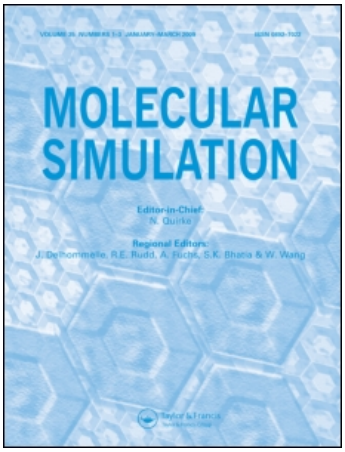

Molecular Simulation
Publication details, including instructions for authors and subscription information:
http://www.informaworld.com/smpp/title~content=t713644482

Molecular dynamics simulations of Ac-3Aib-Cage-3Aib-NHMe

Parvesh Singh[a]; Parul Sharma[a]; Krishna Bisetty[a]; Juan J. Perez[b]
[a] Department of Chemistry, Durban University of Technology, Durban, South Africa [b] Department d' Enginyeria Quimica, UPC, ETS d'Enginyers Industrials, Barcelona, Spain

Online publication date: 24 November 2010

To cite this Article Singh, Parvesh , Sharma, Parul , Bisetty, Krishna and Perez, Juan J.(2010) 'Molecular dynamics simulations of Ac-3Aib-Cage-3Aib-NHMe', Molecular Simulation, 36: 13, 1035 — 1044
To link to this Article: DOI: 10.1080/08927022.2010.501797
URL: http://dx.doi.org/10.1080/08927022.2010.501797

Molecular Simulation
Vol. 36, No. 13, November 2010, 1035–1044

Taylor & Francis
Taylor & Francis Group

Molecular dynamics simulations of Ac-3Aib-Cage-3Aib-NHMe

Parvesh Singh[a], Parul Sharma[a], Krishna Bisetty[a]* and Juan J. Perez[b]

[a]*Department of Chemistry, Durban University of Technology, Steve Biko campus, P.O. Box 1334, Durban 4000, South Africa;*
[b]*Department d' Enginyeria Quimica, UPC, ETS d'Enginyers Industrials, Avenue Diagonal 647, 08028 Barcelona, Spain*

(*Received 16 March 2010; final version received 14 June 2010*)

Solvents play a stabilising role with the more stable conformations obtained in polar solvents than *in vacuo*. We investigate to what extent the structural propensities of the pentacyclo-undecane (PCU) cage polypeptide chain of the type Ac-3Aib-Cage-3Aib-NHMe are influenced in implicit water and in explicit solvents: methanol (MEOH), dimethyl sulphoxide (DMSO) and TIP3P water. The sampling of the α-helical conformations of the PCU cage polypeptide was investigated using the in-house modified PARM94 force-field parameters. Analysis of 50 ns molecular dynamics (MD) simulations revealed a tendency of the PCU cage polypeptide to assume bent structures, especially in polar solvents. The choice of solvents was designed to relate the simulations to physiological conditions. The individual amino-isobutyric acid residues predominantly sampled the right-handed and left-handed 3_{10}-helical conformations, indicating that the helical conformations are preferred in all four environments (*in vacuo*, MEOH, water and DMSO). Additionally, the 100 ns replica exchange MD (REMD) simulations of the PCU cage polypeptide in implicit water revealed more conformational variety present than in explicit solvents, and is more consistent with previous theoretical studies on the PCU cage residue. The present theoretical results may help in rationalising experimental results on these PCU cage polypeptides, and definitely show the importance of a dynamical approach for a correct interpretation and prediction of the conformational behaviour of the PCU cage molecules in different environments.

Keywords: pentacyclo-undecane cage polypeptides; conformational analysis; α-helical; molecular dynamics; polar solvent

Introduction

It is well known that molecular dynamics (MD) simulations have become a powerful tool for studying the structure and dynamics of biologically important molecules [1,2]. With increasing computational power, larger and larger systems can now be simulated for increasingly longer periods of time. In the past, MD simulations hardly exceeded a few picoseconds, but today, trajectories of nanoseconds are widely reported [3]. Literature studies revealed that solvents play a pivotal role in decreasing the free energy difference between the conformations that differ by large energies on the vacuum surface, and thus lowers the barriers separating these conformations. From these studies, it has become apparent that water-specific interactions are very important in the structural and functional aspects of biopolymer chemistry. Tobias and Brooks [4] reported a remarkable change in the conformational stability of the alanine dipeptide when MD simulations performed in the gas phase were compared with those obtained in the solvent phase.

Reviews on the crystal structure of peptides containing the amino-isobutyric acid (Aib) residues [5–7] have confirmed a helical preference in their conformation. Accordingly, this structural preference has been systematically investigated against the Aib content and the position of the Aib residues along the pentacyclo-undecane (PCU) cage polypeptide chain. The prediction of the accessible conformations of polypeptides containing several Aib units has been a challenge for theoretical methods, because a delicate balance between the different contributions to the interatomic interactions may favour, depending on various factors, different types of helices. In an earlier molecular mechanical study of poly-Aib, Prasad and Sasisekharan [8] predicted the 3_{10}-helix and α-helix to be the most favourable structures, the latter being more stable by about 3 kcal mol^{-1} per Aib residue. However, in a more recent study, Patterson et al. [9] studied oligomers of Aib up to three units using the empirical conformational energy program for peptides (ECEPP) force field [10]. The results indicated that the minimum-energy conformations correspond to a 3_{10}-helix. Nevertheless, the preference of this helix was only achieved by imposing a constraint on the Cα atom; without this constraint, the α-helix appeared to be more stable. Barone et al. [11] investigated the conformational behaviour of Aib by *ab initio* and empirical methods. They found that the relative stability of the C_5, C_7 and helical conformations strongly depends on the force-field parameterisation when molecular mechanical calculations are performed.

*Corresponding author. Email: bisettyk@dut.ac.za

ISSN 0892-7022 print/ISSN 1029-0435 online

DOI: 10.1080/08927022.2010.501797
http://www.informaworld.com

In recent studies [12–16], we investigated the intrinsic conformational properties of (*R*)-8-amino-pentacyclo[5.4.0.0^{2,6}.0^{3,10}.0^{5,9}] undecane-8-carboxylic acid monopeptide (PCU cage monopeptide), using molecular mechanics, *ab initio* and DFT methods. Our initial gas-phase study revealed the presence of four low-energy conformers, C_{7ax}, C_{7eq}, 3_{10} and α_L located on the conformational space of the PCU cage residue (**1**). These studies also indicated that the peptide sequences are effective at stabilising the *trans* conformer of the amide bonds between residues $(i + 1)$ and $(i + 2)$ which satisfy the criteria for reverse-turns and with a strong tendency to promote β-turns [17]. Our continuous interest in the PCU cage peptide chemistry, coupled with their widely reported potential bioactivity [18–20], prompted us to explore the conformational profile of PCU cage peptides under different environmental conditions. In this paper, we wish to report the conformational studies of PCU cage polypeptide chain of the type Ac-3Aib-Cage-3Aib-NHMe carried out *in vacuo* and in explicit solvents, viz. dimethyl sulphoxide (DMSO), methanol (MEOH) and TIP3P. The selection of the organic solvents for the present investigations has been made to mimic the dynamic behaviour of these polypeptides under physiological conditions. Accordingly, our aim in this paper is to ascertain the impact of the presence of PCU cage residues in Aib polypeptide chains of the type Ac-3Aib-Cage-3Aib-NHMe using MD simulations in different environments. Thus, it is expected that the inclusion of the intervening three Aib residues on either side of the PCU cage residue **(1)** would display distinct conformational preferences and hence provide additional information about the conformational characteristics of PCU cage polypeptides in different environments. Additionally, replica exchange MD (REMD) methodology has also been used to explore the conformational profile of the PCU cage polypeptide using the implicit model (GB^{OBC}) of the water solvent.

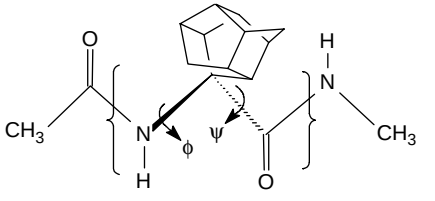

(**1**) Ac-PCU Cage-NHMe

Computational methodology

MD simulations

The MD trajectories were carried out within the framework of molecular mechanics, using the in-house modified all-atom PARM94 force-field parameters from AMBER 8.0 [21,22], and 3Aib-Cage-3Aib-NHMe was built using the ANTECHAMBER module [23] of AMBER. The MD simulations were carried out *in vacuo*, water TIP3P model [24], DMSO and in a box of MEOH molecules [21]. An extended conformation of 3Aib-Cage-3Aib-NHMe was used as the starting structure. The system was then minimised using 10,000 steps of steepest descent, followed by a subsequent minimisation using the conjugate gradient algorithm until a convergence of the

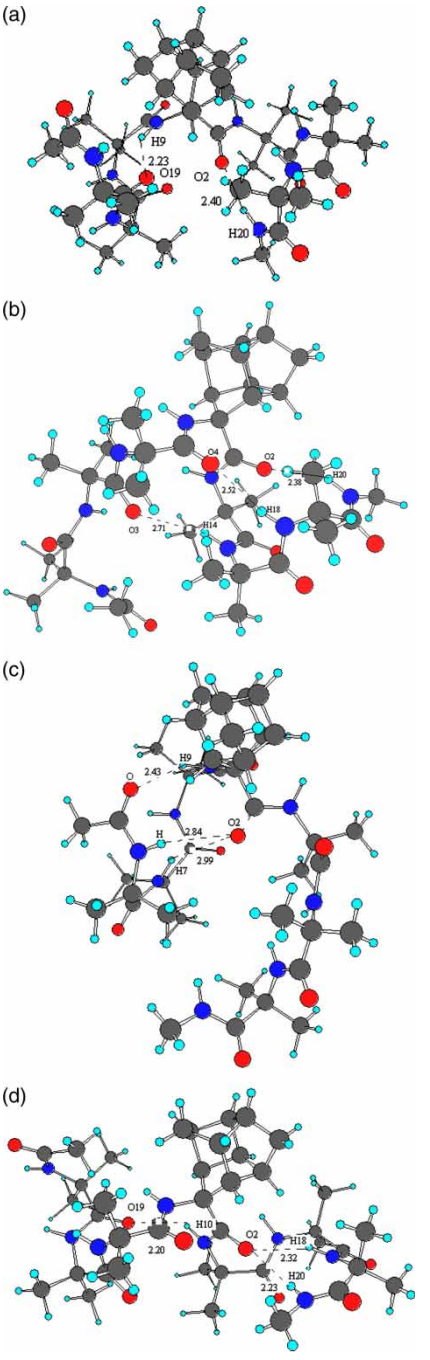

Figure 1. Average structures taken from 50 ns MD trajectories for Ac-3Aib-Cage-3Aib-NHMe in (a) *in vacuo*, (b) methanol (MEOH), (c) DMSO and (d) water (TIP3P).

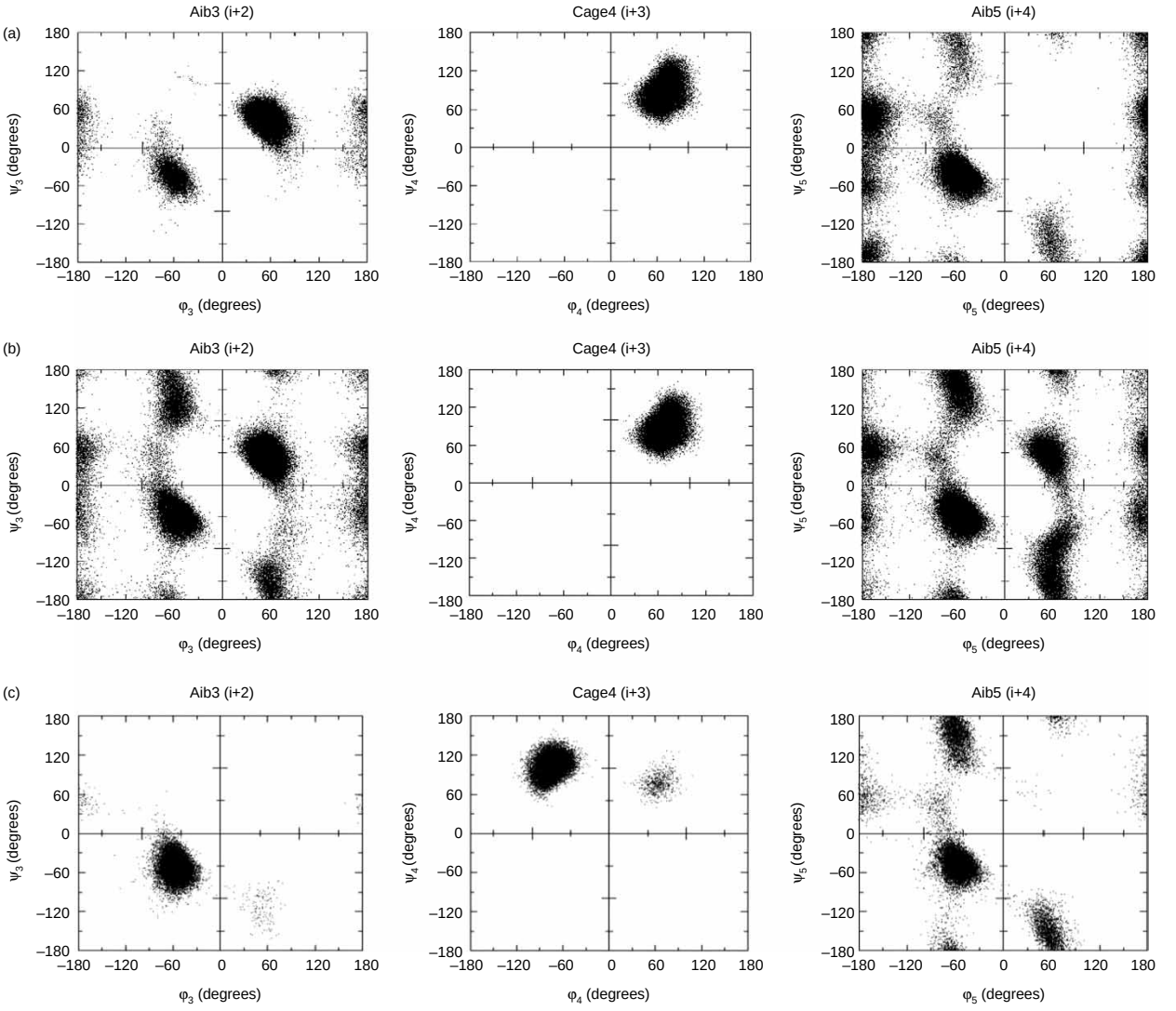

Figure 2. Ramachandran plots for Ac-3Aib-Cage-3Aib-NHMe in (a) water (TIP3P), (b) MEOH and (c) DMSO.

gradient norm was lower than 0.001 kcal mol^{-1}Å. The molecule was placed into a rectangular box of $36 \times 35 \times 38$ Å^3 within the TIP3P water. The minimisation of these new systems were completed when the convergence criteria (0.001 kcal mol^{-1}Å) was fulfilled. Thereafter, periodic boundary conditions [25] were introduced and the structure was allowed to equilibrate for 500 ps at a temperature of 300 K, with pressure set to 1 bar. SHAKE was used on bonds involving hydrogen atoms with a time step of 2 fs. After the first equilibration phase, the particle-mesh Ewald method [26] was applied with a grid spacing of approximately 1 Å. The equilibration phase involved a single MD trajectory run for 50 ns under these conditions. Similar protocols were used to carry out MD simulations of 3Aib-Cage-3Aib-NHMe in MEOH and DMSO.

REMD simulations

An extended structure of 3Aib-Cage-3Aib-NHMe was used as the initial structure. For the generalised born (GB) approximation, a default bond radius [27–29] was used. REMD was performed using implicit model of solvent based on the GB approximation: Onufriev, Bashford and Case (GB^{OBC}) implementations [30]. The dielectric constant around the peptide (internal dielectric constant) was set to 1 and the external dielectric constant set to 80, corresponding to water. Prior to the REMD simulations, standard MD simulations were performed for 5 ns at each temperature (in the present study, 10 replicas were used and the temperature of each replica was set at: 269, 300, 334, 371, 412, 457, 507, 562, 622 and 690 K). In all MD and REMD simulations, the time step was set to 0.2 fs, and

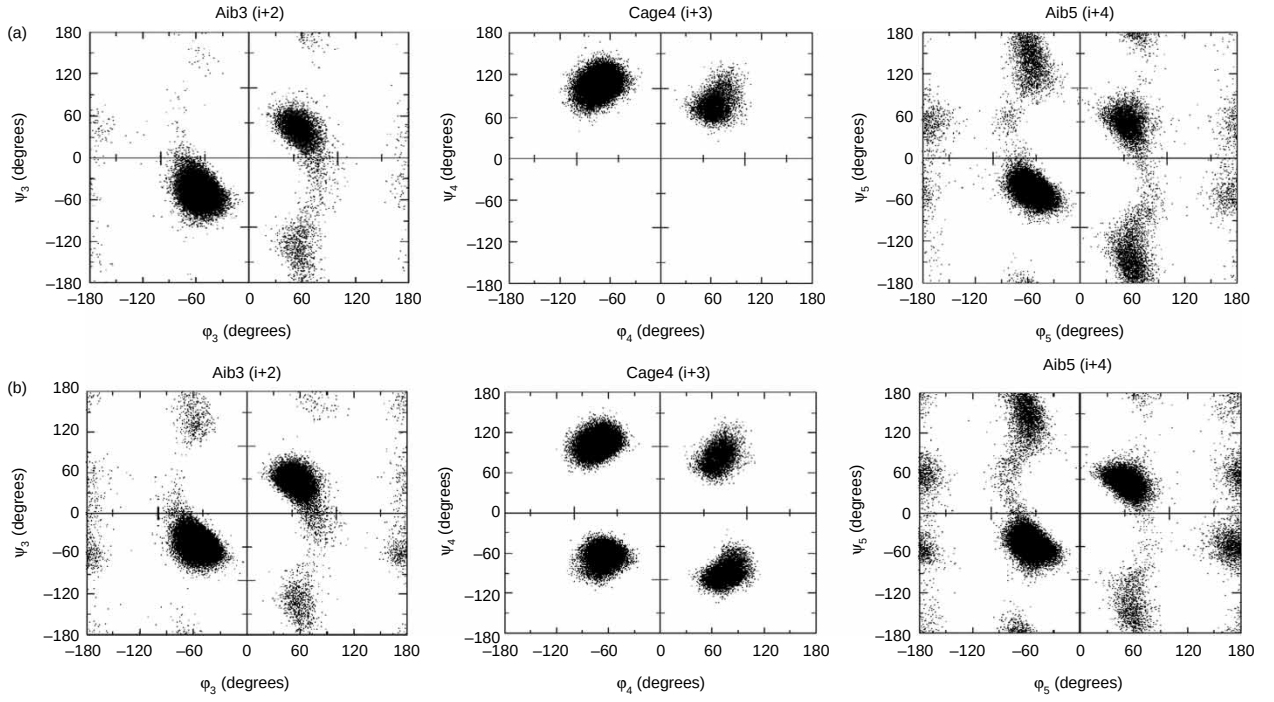

Figure 3. Ramachandran plots for Ac-3Aib-Cage-3Aib-NHMe (a) *in vacuo* and (b) implicit water (REMD).

the SHAKE method was to used constrain the all hydrogen atoms. The temperature during MD simulations was regulated by the Langevin thermostat [27–29], and the GB surface area solvation model was used. Each replica was simulated simultaneously and independently at different temperatures (269–690 K range). The replica exchange was performed every 2 ps for 50,000 steps during the REMD simulations. All trajectories were carried out using the PTRAJ module of AMBER 8.0 [21].

Classification of structures

Analysis of the all trajectories was carried out using the classification of structures (CLASICO) software [31] which permits to monitor the formation–destruction of secondary structures during the folding process, as well as the characterisation of the group of structures that represent the folded molecule. The characterisation of β-turn profile for each of the trajectories was carried out using the procedure described by Corcho and co-workers [32,33]. This procedure also permits to identify the different conformational patterns attained by the peptide, as well as to compare differences of the conformational space sampled using different computational methods.

Results and discussion

A visual inspection of the snapshots for the average structures shown in Figure 1(a)–(d) (stripped off solvent molecules in 1(b)–(d)) taken from the 50 ns MD trajectories reveal that the backbone atoms of Ac-3Aib-Cage-3Aib-NHMe are closely packed with side chains projecting outwards, typical of β-turn structures [34]. However, a closer inspection of Figure 1(b) and (d) indicates that the molecules are very closely packed in the polar solvents, suggesting the presence of strong intramolecular hydrogen bonds. In addition, the extent of intramolecular hydrogen bonding is also greater in polar solvents (MEOH and water). The type of conformations in polar solvents was found to be α-helices established on the basis of intramolecular H-bonds formed between residues (2 and 6) and between residues (3 and 7) in MEOH, and between residues (1 and 5) in the case of water. On the other hand, 3_{10}-helical conformations were found *in vacuo* and in DMSO, showing the formation of H-bonds between their residues (1 and 4), as depicted in Figure 1(a) and (c), respectively.

The conformational results for the residues occupying positions $(i + 2)$ to $(i + 4)$, respectively, are presented in the Ramachandran plots in Figures 2 and 3. A similarity in the conformational preferences exhibited by each of the Aib segments as well as the PCU cage residue is observed. However, the most striking feature is the restricted nature of the conformational space exhibited by the PCU cage residue in the $(i + 3)$ position. This corresponds to the transformation of initial α_L conformation into energetically more favourable C_{7eq} conformation after initial 5 ns of MD (Figure 2(c)) in DMSO. However, in the case of

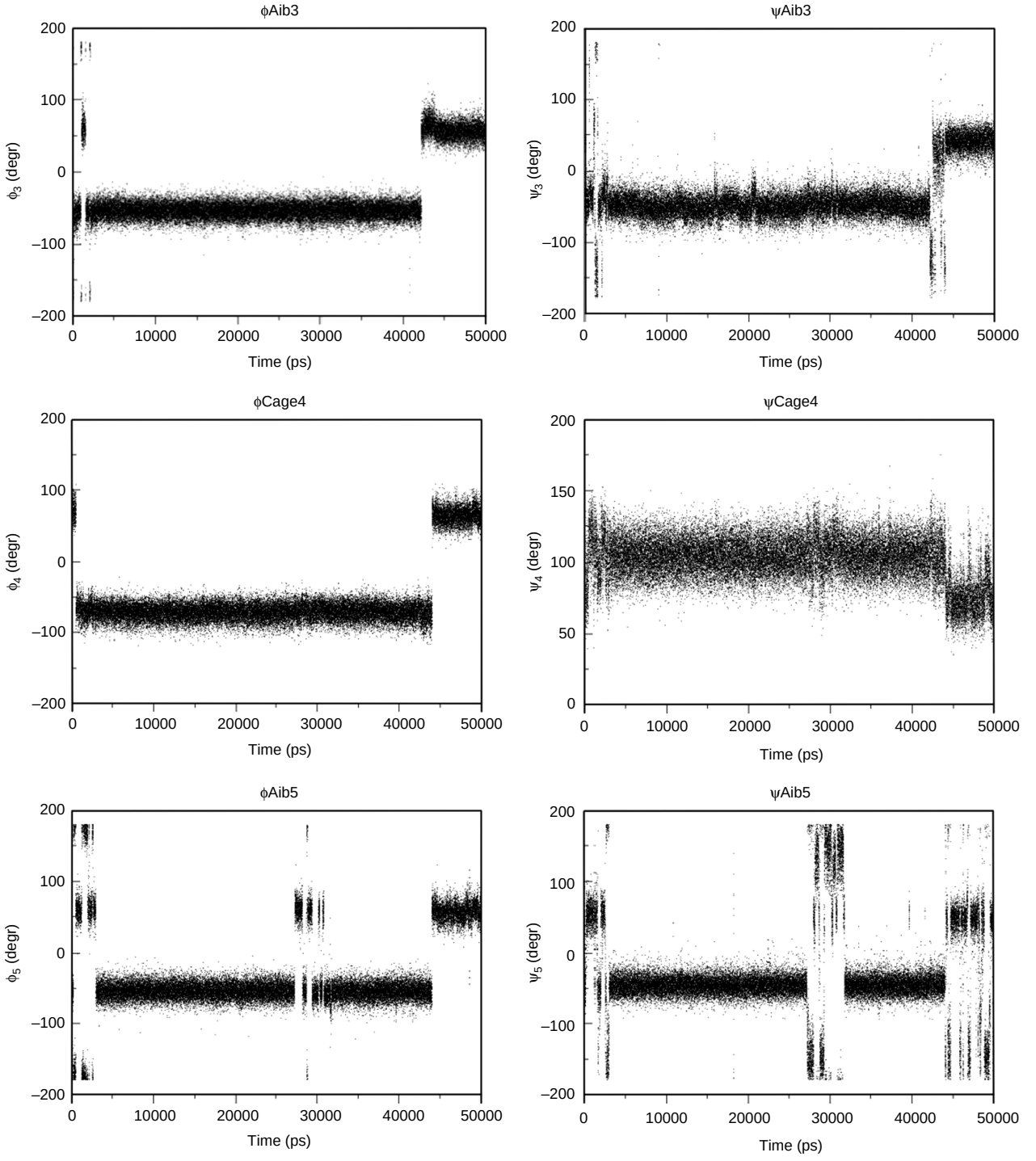

Figure 4. Backbone torsion angles Ac-3Aib-Cage-3Aib-NHMe *in vacuo*.

vacuo simulations, the initial conformation α_L changed into C_{7eq} after initial 4 ns and retained the same conformation until 40 ns after which some of the conformations (approx. 40%) reverted back to α_L (Figure 3(a)). Specifically, the conformational profile of the PCU cage residue fluctuates between α_L and C_{7eq} *in vacuo*. On the other hand, helical (α_L) conformations were preserved in polar solvents such as water and MEOH (Figure 2(a) and (b)). The observed retention of helical conformation in polar solvents could be explained by the hydrophobic–hydrophilic repulsion between the PCU cage residue and the solvent molecules, thus resulting in bent and stable structures due to the facile nature of the intramolecular hydrogen bonding (Figure 1(b) and (d)).

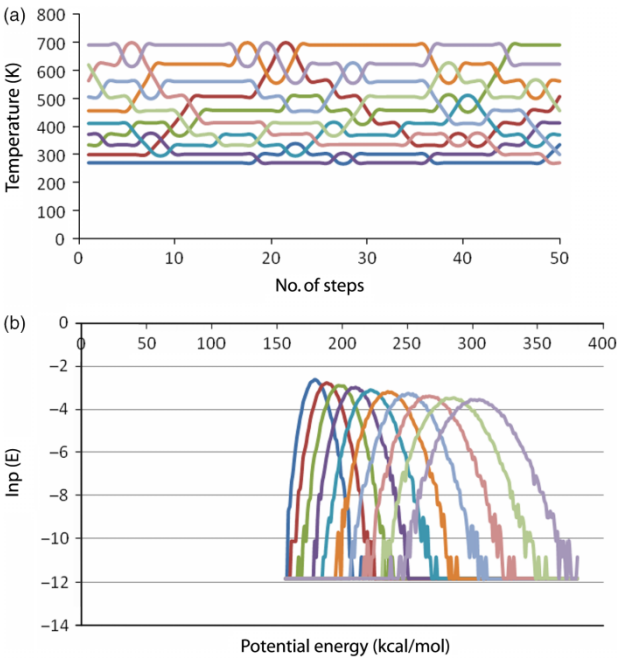

Figure 5. Time series of temperature exchanges for the initial 50 steps of REMD (a) and the canonical probability distributions of the total potential energy of Ac-3Aib-Cage-3Aib-NHMe obtained from the REMD simulation at 10 temperatures (b). The distributions in (b) correspond to the following temperatures (from left to right): 269, 300, 334, 371, 412, 457, 507, 562, 622 and 690 K.

Moreover, the trapping of α_L conformations in their local energy minima could be another reason for the observed behaviour of the PCU cage residue in the polar solvents. In comparison to polar solvents, a greater conformational flexibility is observed *in vacuo* and in the non-polar solvent DMSO, resulting in the conversion of α_L into comparatively more stable C_{7eq} conformations.

The plots in Figure 4 suggest fluctuations and movement in the backbone torsion angles along the MD trajectories. The graphs indicate that the backbone torsion angles ($\phi = 70°$, $\psi = 80°$) of the PCU cage (*in vacuo*) in the $(i + 3)$ position change immediately after 4 ns of MD run, and remain relatively fixed ($\phi = -60°$, $\psi = 100°$) up to 45 ns adopting a C_{7eq} conformation, after which they revert back to the original α_L conformation ($\phi = 70°$, $\psi = 80°$). However, in the case of DMSO, the backbone torsion angles remain relatively fixed ($\phi = -60°$, $\psi = 100°$) throughout the 50 ns trajectory, after getting transformed from their original angles ($\phi = 70°$, $\psi = 80°$) in the first 5 ns, adopting a C_{7eq} conformation as depicted in Figure A (see Supplementary Data, available online). On the other hand, the dihedral angles do not fluctuate to a considerable extent in water and MEOH as shown in Figures B and C, respectively (see Supplementary Data, available online), thus restricting the left-handed α-helical conformation of the PCU cage residue in both polar solvents. In addition, a broader range of ϕ and ψ backbone torsion angles ($-180°$ to $+180°$) is observed for the Aib residues for the initial 3 ns trajectory. A broader fluctuation in the backbone torsion angles has been found for the seventh residue of the 3Aib-Cage-3Aib-NHMe peptide, in the case of MEOH and water, as depicted in Figures B and C, respectively (see Supplementary Data, available online).

Overall, these results revealed that the replacement of Aib by the PCU cage residue in the $(i + 3)$ position has a marked influence on the overall patterns of the ψ backbone torsion angles of C-terminal Aib residues. The significance of this result is attributed to the fact that the presence of the bulky PCU cage structure imposes an additional strain on ψ backbone torsion compared to the less bulky methyl groups positioned on each of the Cα atoms in Aib.

REMD simulations, on the other hand, emerged as an efficient technique for overcoming the multiple-minima problem so that a random walk on the energy surface may be realised [35–37]. The random walk allows the simulation to pass any energy barrier and to sample a much wider energy surface than by conventional simulations. Accordingly, REMD simulations of 100 ns trajectories were performed on the Ac-3Aib-Cage-3Aib-NHMe in implicit water. Figure 5 shows the time series of temperature exchanges for the initial 50 steps of 100 ps trajectory along with the canonical probability distributions of the total potential energy of Ac-3Aib-Cage-3Aib-NHMe. Clearly, a random walk in the 'temperature space' between low and high temperature (Figure 5(a)) was realised. In Figure 5(b), the overlaps between all neighbouring pairs of distributions indicate a sufficient number of replica exchanges between pairs of replicas, suggesting that the present REMD simulations were indeed efficient. The conformational results obtained from one of the replicas (for 300 K) occupying positions $(i + 2)$ to $(i + 4)$, respectively, are presented in the Ramachandran plots shown in Figure 3(b). The remaining plots for this study are not included in this paper. Although a similarity in the conformational preferences exhibited by each of the Aib residues is observed, a major difference has been observed in the case of the PCU cage residue where the conformational space was found to be well explored. The PCU cage residue was found to occupy all the conformational spaces in the Ramachandran plots confirming the existence of C_{7ax}, C_{7eq}, 3_{10} and α_L conformations. Interestingly, these results were found to be in complete agreement with our previously reported theoretical results [12–16] performed on the individual PCU cage residue.

Figure 6(a)–(e) shows the rate of new patterns characterised along the sampling process for every snapshot in each of the MD and REMD trajectories as described in the Method section. Accordingly, 44223,

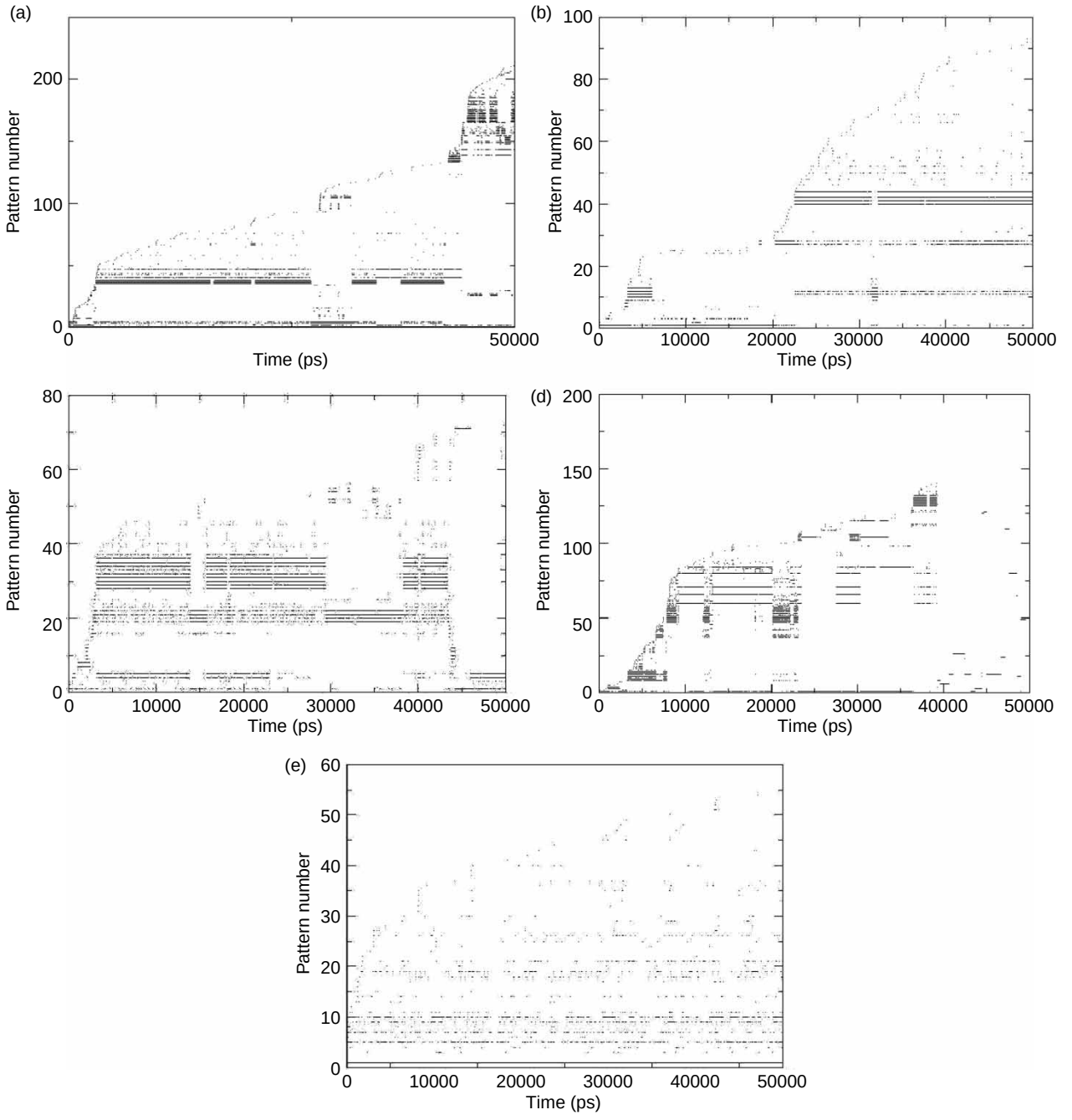

Figure 6. Evaluation of new patterns along the trajectories for the peptide Ac-3Aib-Cage-3Aib-NHMe (a) *in vacuo*, (b) DMSO, (c) TIP3P, (d) MEOH and (e) implicit water (REMD).

39546, 45239 and 47239 new conformational patterns corresponding to 50,000 snapshots of the four MD trajectories and 79236 new patterns were identified after 100,000 snapshots of REMD simulations. These plots provide a broad estimation of the performance of the different protocols in sampling new patterns. A visual inspection of Figure 6 indicates that the simulations are not searching for any more new patterns, and probably have reached convergence. In the case of polar solvents (MEOH and TIP3P), although the conformations of peptide seem to get trapped in regions of the conformational space (Figure 6(c) and (d)) at certain levels, new patterns appeared in a stable manner for the remainder of the trajectories (Figure 6(a), (b) and (e)), suggesting their less restrictive nature of exploring the conformational space.

Moreover, the secondary structure analysis for every snapshot in each trajectory of the five trajectories using a two-residue window [32,33] is depicted in Figure 7(a)–(e).

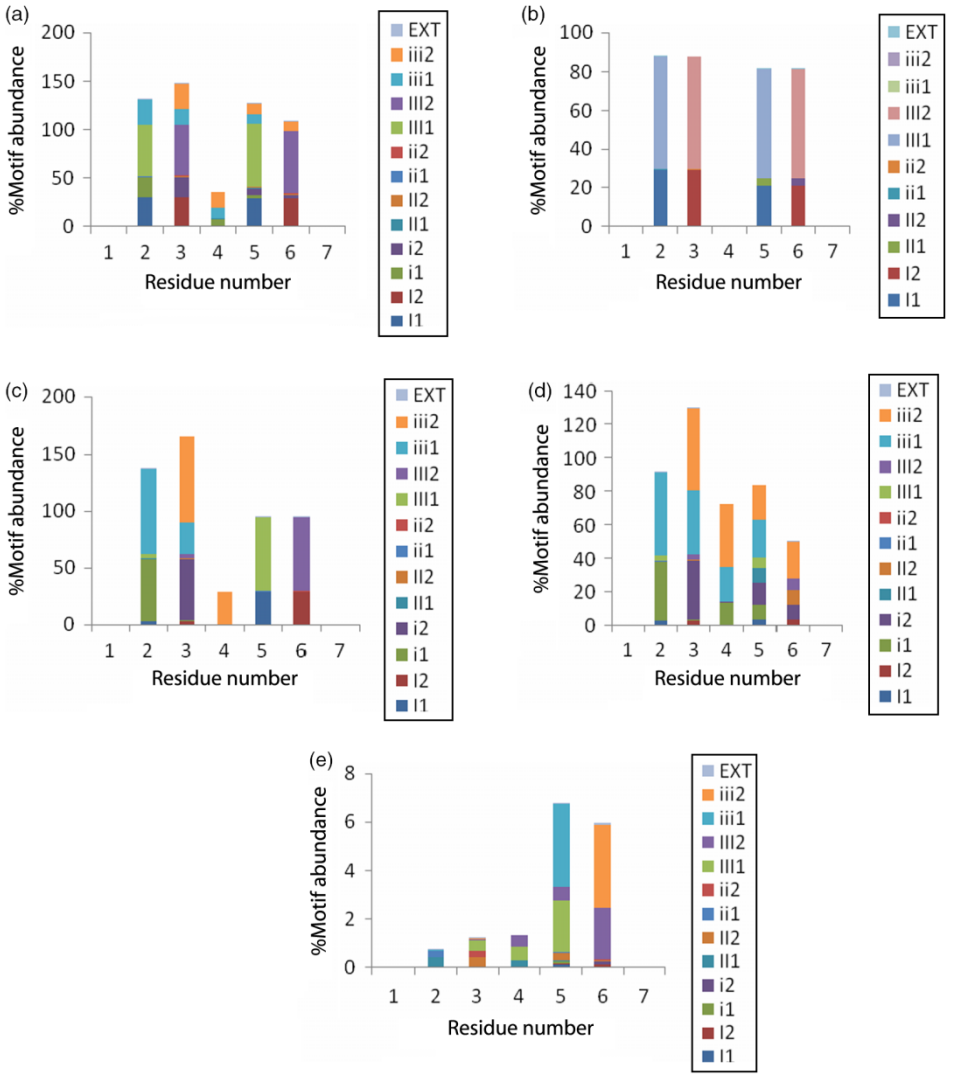

Figure 7. β-Turn profiles obtained for the peptide Ac-3Aib-Cage-3Aib-NHMe (a) *in vacuo*, (b) DMSO, (c) TIP3P, (d) MEOH and (e) implicit water (REMD).

Specifically, the conformational motifs obtained *in vacuo* (Figure 7(a)) show the predominance of β-turn type III between residues 2 and 6 with a low propensity between residues 4 and 5. To a minor extent, β-turn type I was also observed between residues 2 and 3, and 5 and 6. Although a similar β-turn profile can be observed in the case of DMSO (Figure 7(b)), the extent of β-turns was almost negligible between residues 3 and 4. In the case of TIP3P, the peptide adopts a β-turn of type III between residues 2 and 4 (Figure 7(c)) and type III between residues 2 and 3, and 5 and 6. In MEOH (Figure 7(d)), a β-turn of type III was found to be predominant between residues 2 and 6 with a low propensity between residues 5 and 6. On the other hand, the PCU cage polypeptide exhibits mainly β-turn type III between residues 5 and 6 with a low propensity between residues 3 and 4. Surprisingly, the extent of β-turns, observed in the case of REMD, was low (~7%) in contrast to other environments used for the MD simulations.

Overall, these results reveal that PCU cage polypeptide predominantly adopts a β-turn type III conformation, irrespective of the environment used for the simulations. Although the polypeptide chain has a strong tendency to form β-turns, the PCU cage residue disrupts this tendency in all solvents with the exception of MEOH, and to a lesser extent in TIP3P. Hence, this type of information could be invaluable in determining the bioactive conformation of PCU cage polypeptides in the future.

Conclusions

Our results confirm the preference of the PCU cage peptide to adopt bent structures, especially in the polar solvents (MEOH and water). Interestingly, the explicit MD

simulations for MEOH and water were unable to sample all four low-energy conformers (C_{7ax}, C_{7eq}, 3_{10} and α_L) previously reported for the cage residue. However, these results support the tendency of Ac-3Aib-Cage-3Aib-NHMe to adopt bent conformations, a feature that could be invaluable to the general field of peptidomimetics. REMD simulation, on the other hand, of the PCU cage peptide was able to sample all the four low-energy conformers under implicit water condition. Moreover, analysis of the secondary structure profile for the different trajectories also predicts the predominant existence of β-turn type III conformations. This information could be helpful to determine the bioactive conformation of this kind of polypeptides and thus, could play informative role in the design of new peptide-mimicking drugs. Our results confirm that the seven-residue peptide analogues may be utilised as places for folding back into a polypeptide chain, thus enabling the formation of a cyclic chain structure.

Acknowledgements

K.B. gratefully acknowledges financial support from the Durban University of Technology and the National Research Foundation (GUN No. 2069745).

References

[1] W.F. van Gunsteren and A.E. Mark, *On the interpretation of biochemical data by molecular dynamics computer simulation*, J. Biochem. 204 (1992), pp. 947–961.

[2] M. Karplus and G.A. Petsko, *Molecular dynamics simulations in biology*, Nature 347 (1990), pp. 631–639.

[3] S. Weerasinghe, P.E. Smith, V. Nohan, Y.K. Cheng, and B.M. Petit, *Nanosecond dynamics and structure of a model DNA triple helix in saltwater solution*, J. Am. Chem. Soc. 117 (1995), pp. 2147–2158.

[4] D.J. Tobias and C.L.I. Brooks, *Conformational equilibrium in the alanine dipeptide in the gas phase and aqueous solution: A comparison of theoretical results*, J. Phys. Chem. 96 (1992), pp. 3864–3870.

[5] C. Toniolo, M. Crisma, F. Formaggio, E. Benedetti, A. Santini, R. Iacovino, M. Saviano, B. DiBlasio, C. Pedone, and J. Kamphuis, *Preferred conformation of peptides rich in alicylic $C^{\alpha,\alpha}$-disubstituted glycines*, Biopolymers 40 (1996), pp. 519–522.

[6] R. Bosch, G. Jung, H. Schmitt, G.M. Sheldrick, and W. Winter, *Peptide structures of the alamethicin sequence: The C-terminal $\alpha/3_{10}$ helical nonapeptide and two pentapeptides with opposite 3_{10} helicity*, Angew. Chem. Int. Ed. Engl. 23 (1984), pp. 450–453.

[7] I.L. Karle, A. Banerjee, and P. Balaram, *Design of two-helix motifs in proteins: Crystal structure of a system of linked helices of opposite chirality and a model helix-linker peptide*, Fold Des. 2 (1997), pp. 203–210.

[8] B.V.V. Prasad and V. Sasisekharan, *A case study of the conformation of poly (α-aminoisobutyric acid): α- or 3_{10}-Helix*, Macromolecules 12 (1979), pp. 1107–1110.

[9] Y. Patterson, S.M. Rumsey, E. Benedetti, G. Nemethy, and H.A. Scheraga, *Sensitivity of polypeptide conformation to geometry. Theoretical conformational analysis of oligomers of α-aminoisobutyric acid*, J. Am. Chem. Soc. 103 (1981), pp. 2947–2955.

[10] F.A. Momany, R.F. McGuire, A.W. Burgess, and H.A. Scheraga, *Energy parameters in polypeptides. VII. Geometric parameters, partial atomic charges, nonbonded interactions, hydrogen bond interactions, and intrinsic torsional potentials for the naturally occurring amino acids*, J. Phys. Chem. 79 (1975), pp. 2361–2381.

[11] V. Barone, F. Fraternalli, and P.L. Cristinziano, *Sensitivity of peptide conformation to methods and geometrical parameters. A comparative* ab initio *and molecular mechanics study of oligomers of α-aminoisobutyric acid*, Macromolecules 23 (1990), pp. 2038–2045.

[12] K. Bisetty, J. Gomez-Catalan, C. Aleman, E. Giralt, H.G. Kruger, and J.J. Perez, *Computational study of the conformational features of the (R)-8-amino-pentacyclo (5.4.0.0^{2,6}.0^{3,10}.0^{5,9}) undecane-8-carboxylic acid monopeptide*, J. Pept. Sci. 10 (2004), pp. 274–284.

[13] K. Bisetty, F.J. Corcho, J. Canto, H.G. Kruger, and J.J. Perez, *Conformational analysis of small peptides of the type Ac–X–NHMe, where X=Gly, Ala, Aib and Cage*, J. Mol. Struct. (Theochem) 731 (2005), pp. 127–137.

[14] K. Bisetty, F.J. Corcho, J. Canto, H.G. Kruger, and J.J. Perez, *A theoritical study of pentacyclo-undecane cage peptides of the type (Ac-X-Y-NHMe)*, J. Pept. Sci. 12 (2006), pp. 92–105.

[15] K. Bisetty, F.J. Corcho, J. Canto, H.G. Kruger, and J.J. Perez, *Simulated annealing study of the pentacyclo-undecane cage amino acid tripeptides of the type [Ac-X-Y-Z-NHMe]*, J. Mol. Struct. (Theochem) 759 (2006), pp. 145–157.

[16] K. Bisetty, H.G. Kruger, and J.J. Perez, *A molecular dynamics study of the pentacyclo-undecane (PCU) cage polypeptides of the type Ac-3Ala-Cage-3Ala-NHMe*, Mol. Simul. 33 (2007), pp. 1105–1108.

[17] G.D. Rose, L.M. Gierasch, and J.A. Smith, *Turns in peptides and proteins*, Adv. Protein Chem. 37 (1985), pp. 1–9.

[18] C.J. Noren, S.J. Anthoney-Cahill, M.C. Griffith, and P.G. Schultz, *A general method for site-specific incorporation of unnatural amino acids into proteins*, Science 224 (1989), pp. 182–188.

[19] J.R. Roesser, M.S. Chorghade, and S.M. Hecht, *Ribosome catalyzed formation of an abnormal peptide analog*, Biochemistry 25 (1986), pp. 6361–6365.

[20] S. Hanessian, G. McNaughton-Smith, H.G. Lombart, and W.D. Lubell, *Design and synthesis of conformationally constrained amino acids as versatile scaffolds and peptide mimetics*, Tetrahedron 53 (1997), pp. 12789–12854.

[21] D.A. Case, T.A. Darden, T.E.III, Cheatham, C.L. Simmerling, J. Wang, R.E. Duke, R. Luo, K.M. Merz, B. Wang, D.A. Pearlman, M. Crowley, S. Brozell, V. Tsui, H. Gohlke, J. Mongan, V. Hornak, G. Cui, P. Beroza, C. Schafmeister, J.W. Caldwell, W.S. Ross, and P.A. Kollman, *AMBER*, 8, University of California, San Francisco, 2004.

[22] S.J. Weiner, P.A. Kollman, D.A. Case, U.C. Singh, C. Ghio, G. Alagona, S. Profeta, Jr, and P.J. Weiner, *A new force field for molecular mechanics simulation of nucleic acids and proteins*, J. Am. Chem. Soc. 106 (1984), pp. 765–784.

[23] J. Wang, R.M. Wolf, J.W. Caldwell, P.A. Kollamn, and D.A. Case, *Development and testing of general amber force field*, J. Comput. Chem. 25 (2004), pp. 1157–1174.

[24] D.M. York, T.A. Darden, and L.G. Pedersen, *The effect of long-range electrostatic interactions in simulations of macromolecular crystals: A comparison of the Ewald and truncated list methods*, J. Chem. Phys. 99 (1993), pp. 8345–8348.

[25] T. Darden, D. York, and L. Pedersen, *Particle mesh Ewald: An N-log (N) method for Ewald sums in large systems*, J. Chem. Phys. 98 (1993), pp. 10089–10092.

[26] A. Bondi, *Van der Waals volumes and radii*, J. Phys. Chem. 68 (1964), pp. 441–452.

[27] X. Wu and B.R. Brooks, *Self-guided Langevin dynamics simulation method*, Chem. Phys. Lett. 381 (2003), pp. 512–518.

[28] H.C. Andersen, *Molecular dynamics simulations at constant pressure and/or temperature*. J. Chem. Phys. 72 (1980), pp. 2384–2393.

[29] R.W. Pastor, B.R. Brooks, and A. Szabo, *An analysis of the accuracy of Langevin and molecular dynamics algorithms*. Mol. Phys. 65 (1988), pp. 1409–1419.

[30] A. Onufriev, D. Bashford, and D.A. Case, *Exploring native states and large-scale conformational changes with a modified generalized Born model*, Proteins 55 (2004), pp. 383–394.

[31] *LaFargaCPL: CLASTERIT: Project info*. Available at: https://lafarga.cpl.upc.edu/projects/clusterit.

[32] F. Corcho, J. Canto, and J.J. Perez, *Comparative analysis of the conformational profile of substance P using simulated annealing*

and molecular dynamics, J. Comput. Chem. 25 (2004), pp. 1937–1952.

[33] F. Corcho, P. Mokoena, K. Bisetty, and J.J. Perez, *Molecular dynamics (MD) simulations of VIP and PACAP27*. Biopolymers 91 (2008), pp. 391–400.

[34] K. Möhle, M. Gussmann, A. Rost, R. Cimiraglia, and H.J. Hofmann, *Correlation energy, thermal energy, and entropy effects in stabilizing different secondary structures of peptides*, J. Phys. Chem. 101 (1997), pp. 8571–8574.

[35] R.H. Swendsen and J.-S. Wang, *Replica Monte Carlo simulation of spin-glasses*, Phys. Rev. Lett. 57 (1986), pp. 2607–2609.

[36] K. Hukushima and K. Nemto, *Exchange Monte Carlo method and application to spin glass simulation*, J. Phys. Soc. Jpn. 65 (1996), pp. 1604–1608.

[37] M.C. Tesi, E.J.J. van Rensburg, E. Orlandini, and S.G. Whittington, *Monte Carlo study of the interacting self-avoiding walk model in three dimensions*, J. Stat. Phys. 82 (1996), pp. 155–181.